LIBERTY UNIVERSITY

Montview Liberty University Journal of Undergraduate Research

Volume 7 | Issue 1 Article 1

2020

An Affordable and Portable Palpable System for Sensing Breast Tissue Abnormalities

Cody J. Clarke
Liberty University, cjclarke2@liberty.edu

Proceedings of the ASME 2020 Conference on Smart Materials, Adaptive Structures and Intelligent Systems
SMASIS2020
September 14-16, 2020, Irvine, CA, USA

SMASIS2020-16379

AN AFFORDABLE AND PORTABLE PALPABLE SYSTEM FOR SENSING BREAST TISSUE ABNORMALITIES

Cody J. Clarke, Ephraim F. Zegeye
Liberty University, Lynchburg, VA, USA

ABSTRACT

Due to the high cost of equipment and lack of trained personnel, manual palpation is a preferred alternative breast examination technique over mammography. The process involves a thorough search pattern using trained fingers and applying adequate pressure, with the objective of identifying solid masses from the surrounding breast tissue. However, palpation requires skills that must be obtained through adequate training in order to ensure proper diagnosis. Consequently, palpation performance and reporting techniques have been inconsistent. Automating the palpation technique would optimize the performance of self-breast examination, optimize clinical breast examinations (CBE), and enable the visualization of breast abnormalities as well as assessing their mechanical properties. Various methods of reconstructing the internal mechanical properties of breast tissue abnormalities have been explored. However, all systems that have been reported are bulky and rely on complex electronic systems. Hence, they are both expensive and require trained medical professionals. The methods also do not involve palpation, a key element in CBE. This research aims in developing a portable and inexpensive automated palpable system that mimics CBE to quantitatively image breast lumps. The method uses a piezoresistive sensor equipped probe consisting of an electronic circuit for collecting deformation-induced electrical signals. The piezoresistive sensor is made by spraying microwave exfoliated graphite/latex blend on a latex sheet. Lumps can be detected by monitoring a change in electrical resistance caused by the deformation of the sensor which is induced by abnormalities in the breast tissue. The electrical signals are collected using a microcontroller and a pixelated image of the breast can be reconstructed. The research is still in progress, and this report serves as proof of concept testing by pressing the probe with hand pressure and reconstructing the electrical signals using Microsoft Excel. Four maps were created for qualitatively analyzing the result. The pressure maps clearly display areas where pressure was applied, indicating the potential of the probe in detecting breast tissue abnormalities. The pressure maps show the feasibility for using such a sensor for the application in CBE. Furthermore, a sensor such as this is also possible of detecting the depth and size of masses within breast tissue, which, may lead to a more accurate diagnosis. Better manufacturing, accuracy, precision, and real-time data feeds are areas of future consideration for this project. This project involves knowledge and applications from mechanical, electrical, computational, and materials engineering.

KEYWORDS

Clinical breast examination, palpation, microwave exfoliated expanded graphite, piezoresistance, e-skin, data acquisition, research and development.

1. INTRODUCTION

The development of this palpable sensor is built upon the technology of expanded graphite (EG). An EG-based sensor is the technical sensing device used for the probe. EG-sensors function on the basis of piezoresistance: a change in electrical resistance due to deformation. Sensors of this type have been used in many different applications such as bodily motion detection, wearable e-skins, biomedical devices, strain gauges for large strain applications, and human plantar pressure mapping[1-3]. EG-sensors are so commonly used because of their range in application and their mechanical flexibility [4]. One other major advantage of EG-sensors is the possibility of exerting a precisely quantified mechanical pressure, which avoids misdiagnosis caused by the operator inaccuracy [5]. As compared to typical breast imaging techniques, automated palpation is non-invasive to the human body and does not provide harmful effects of x-ray accumulation in the body [6].

Apart from the medical and biological applications mentioned above, others have explored ways to sense breast tissue abnormalities. It was shown by Landoni et al. [7] that elastosonography is a promising techniques for quantitatively

detecting breast cancer. However, elastosonography leverages the technology of either ultrasound or magnetic resonance imaging (MRI). Again, this proves as another reason for why palpation techniques should further be explored. Research utilizing palpation for tissue characterization was done by Palacio-Torralba et al. [8]. Their research quantitatively diagnosed soft prostate tissue using viscoelastic time-based palpation instrumentation. Yet, it was concluded that further research is needed on indentation depth: an area of investigation in this research. At last, piezoresistive properties were used in the studies of Pandya et al. [9] where piezoresistive microcantilevers were applied to characterize abnormal breast tissue. Their future works look to fabricate an automated electro-mechanical sensor for detecting cancerous breast tissue.

EG-sensors, and other compliant piezoresistive sensors, are commonly fabricated as composites: where a conductive reinforcing phase is embedded or mated with a compliant polymer[10, 11]. The polymer, most often, is one that can be characterized with a relatively low Young's Modulus, such as silicone rubber or latex, therefore giving the sensor its compliant nature. These sensors can be made with a wide range of polymers thus adapting them to a multitude of applications since they may be fabricated flexible, comfortable, shaped, and sized for any use [12].

For applications of EG-sensors such as pressure mapping, the device's primary sensing effect functions on the principle of piezoresistivity: where mechanical deformations due to compressive/tensile stresses induce a change in *only* electrical resistance of the material (no change in electrical potential). This change in electrical resistance is usually very linearly over a large range of pressures [12]. The strain induced by the applied force alters the graphite's band gap. The alteration allows electrons to move more easily or with more difficulty to the conduction band. As a result, the material's electrical resistance is changed since the density of atomic current carriers is changed [13]. A sensor integrated with a data processor, such as a microcomputer, is able to detect the changes in resistance and a pressure map can be reconstructed from the data.

The properties of piezoresistive EG-sensors reveal the possibility for these types of sensors to not only detect pressure but also produce data such as tangible depth and mass size within human tissues. If the possibility of such data can be realized, it may lead to a more accurate diagnosis of breast tissue abnormalities. This would be a revelation in CBE.

The research directed toward the development of an affordable and portable palpable system for detecting breast tissue abnormalities aims to utilize the capabilities of EG piezoresistive sensors to improve CBE. In the end, a probe equipped with an EG-sensor should mimic CBE but be easier to use, be available to a larger array of people groups, and produce reliable data for the depth/size/location of tissue abnormalities.

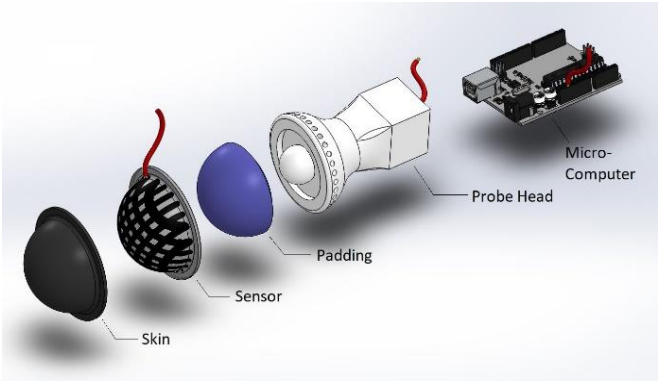

Figure 1: Exploded view of palpating system including, protective skin, EG-sensor, padding, probe head, and microprocessor.

2. MATERIALS AND METHODS

Many measures and processes were used in the development and manufacturing of this piezoresistive breast sensor. The design of the system was developed in three main parts: an EG piezoresistive sensor, a supporting 3D printed probe head, and a micro-processing device for data collection and processing. The development began with research conducted on EG-based sensors and piezoresistivity. From this research, the probe was designed conceptually. A prototypical, research, and development (R&D) approach was heavily used for this process.

2.1 Probe Head Construction

The conceptual ideas for the design of the probe head were modelled virtually using computer aided design (CAD). Many model versions were created. A refined CAD model was physically manufactured by 3D printing the probe head in Acrylonitrile Butadiene Styrene (ABS) plastic.

This current probe head design utilizes a 50.8 mm hemispherical sensing area designed to rest upon an extension grip that fits comfortably in a human hand. The 50.8 mm diameter of sensing area allows for an 8x8 grid of EG sensing strips to be oriented. The handle of the probe head is designed to house the electrical data processing components of the system. The palpating end of the probe head was designed with a smaller hemispherical shape on the interior of the padding to add mechanical rigidity and support to the padding. This support ensures appropriate deformation of the sensor for accurate readings (Fig. 1). Other CAD model variations that were considered incorporated paths for wiring and various methods for supporting and mounting the sensor. Most notably, the size and shape of the probe head was varied; the sensing depth and range of the sensor would be affected by the convex nature of the probe head.

The padding is molded of Ecoflex 00-20 platinum-catalyzed silicone from Smooth-On. Molds, 3D printed in ABS, are used to shape the padding while it cures. The padding gives the sensor the 50.8 mm diametral shape on the palpating end of the probe head.

2.2 Sensor and Electrode Manufacturing

Covering the padding, is the EG-sensor. The sensor is an 8x8 grid of EG sensing strips where 8 of the strips are oriented vertically on the latex skin and the other 8 strips are adhered perpendicular to the first on the other side of the latex skin. The length of each strip varies from approximately 40 mm – 65 mm and approximately 3.5 mm in width. The length depends on where the sensing strip is situated on the probe head. This is because the EG sensing strips follow the arc length contour of the hemispherical design of the sensing area. The strips near the center are longer than the strips located on the edges.

The EG-sensor was manufactured from an EG composite solution that was sprayed to adhere onto a latex skin. The latex skin used was a 50.8 mm white latex party balloon. A latex balloon offers a precise spherical shape with a uniform thickness. The latex balloon was trimmed (with some excess) to a hemispherical shape to stretch over the padding and secure itself and the padding to the probe head.

To manufacture the e-skin sensor, microwave exfoliated EG solution was prepared in a graphite-water solution. This was done by repeatedly microwaving graphene flakes for 30-60 seconds until all the flakes had expanded [10]. To create the solution, 350 ml of deionized (DI) water, 3.5 grams of EG, 2.63 g of Triton x-100, and 25 drops of SE-15 antifoam were mixed mechanically for 10 mins. Triton x-100 and SE-15 antifoam were used in the solution to reduce the amount of foaming during the ultrasonication process. The solution was then sonicated while being mechanically stirred for 30 minutes (3 mins on and 0.5 mins off) in an ice bath at 40% max amplitude of sonication and using the 70% maximum microtip [10]. Triton x-100 surfactant was added during the sonication process because exfoliated graphite is naturally hydrophobic and is not easily suspended in water.

To ensure the solution would adhere to the latex skin, latex was added. In this process, 0.936 g of Castin' Craft Mold Builder latex was added to 12.203 g of EG sonicated solution. The solution was agitated by hand for 30 seconds and then homogenized using a vortex mixer for 1 min.

This EG-latex solution was then sprayed on the latex skin using an airbrush. Prior to spraying, the skin was stretched over the padding of the probe head. A silicone stencil was placed over the skin and a 3D printed stencil was placed over the silicone stencil to secure the entire apparatus. The stencils are 50.8 mm hemispherical domes with 8 parallel slots cut over the circumference to create the 8 EG sensing strips during the airbrush spraying process. Approximately 15 layers of EG-latex solution were sprayed on the skin or until the resistance of each sensing strip was between 5-10 kΩ. At one end of the sensing strips, more solution was added to connect the ends of the 8 strips to create one common terminal.

Electrodes were connected to the end of each of the 8 sensing strips and one electrode at the jointed terminal end. The electrodes are approximately 150 mm in length, where half of the length is carbon braid and the other half is 18-gauge copper strand electrical wire. The carbon end was adhered to the sensing strips using strain gauge grade cyanoacrylate (CA) glue and additional EG solution to ensure good conductivity. The copper end was to be connected to the microprocessor.

The entire grid of sensing strips was then covered in a latex-water solution (3 g of latex with 10 g of DI water). Approximately 40 layers of latex-water solution was sprayed over the entire grid to protect the sensor.

The latex skin was then flipped so that the same sensing strips could be made on the opposing side to complete the sensing grid. The sensing strips on the opposite side of the latex skin were manufactured using the same process as outlined above. On the opposing side, 8 sensing strips and electrodes were attached at a right angle to the original side. This side was also covered in latex to protect it.

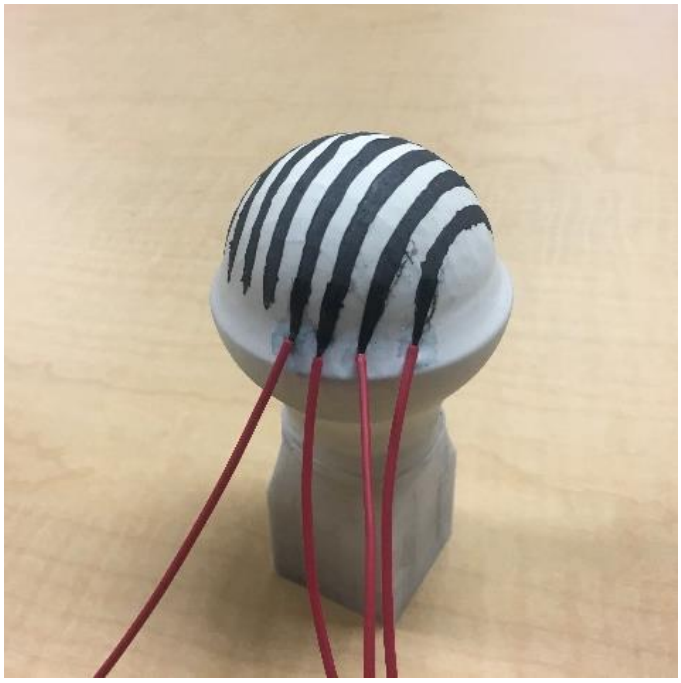

Figure 2: Semi-completed probe head. Photographed after securing some of the electrodes onto the first side of the EG-sensor.

2.3 Data Acquisition and Testing

For testing the sensor, the sensor was connected to a data acquisition (DAQ) system that outputs sensor readings to a log file. The DAQ system is compromised of multiplexers and an *Arduino*. The *Arduino* was used to apply a voltage to the sensing strips, measure the output voltage, convert the output to a digital value, and log the digital values on a PC through a Java application. Voltage is supplied to the system via AA batteries; the Arduino scales down the voltage to approximately 3 V. As discussed previously, the sensor acts as a resistor: when no deformation occurs, the input voltage is the same as the output voltage. When pressure is applied and deformation does occur, the resistance increases and therefore the output voltage increases according to equation (1), where V is voltage in volts, I is current in amperes, and R is resistance in ohms.

$$V = IR \quad (1)$$

For more precise data processing, a cycle was initiated at the start of testing to cycle through each available electrode line (whether it was used or unused). The *Arduino* code converts the input data to gain results, taking the analog voltage from each line and converting it to a digital format.

During testing, four different tests were executed: two baseline tests and two pressured tests. A baseline test must first be executed so that comparative pressure readings may be calculated. When prompted by the user, the set of readings is saved as base values. Now the difference between the base values and new output data (from pressured tests) can be combined. The data collected from the top layer and the bottom layer of the sensor were collected separately. The data from the two layers were summed and stored in matrix form where each summed data point represents a cross point of the sensing strips. A cross point is each instance where two sensing strips overlap perpendicular to one another. This process creates a data point that is associated with each intersecting point of the sensing strips resulting in a data log for the test. The data log is in text document form and was logged on the PC.

With the logged data, the data cross point matrices are organized according to the time they were taken. Data was logged every 200 milliseconds. The earlier conversions performed on the data results in units of volts. Each data cell is assigned a voltage value based on the data at that cross point in the matrix. The cells are color-coordinated according to their data by using conditional formatting. A green color is assigned to sensor areas with no pressure (data cut-off value of 0 mV) and a red color is assigned to areas where maximum pressure was sensed (data cut-off value of 30 mV). A color gradient from green to red was used for the values in between the minimum and maximum values. The color gradient assigned to each cross point of the matrix creates a pressure map. The pressure map is a simple way to visualize and understand the pressure.

The tests were conducted for a length of 5 minutes. For the baseline tests, the sensor was left with no interaction to pressure for 5 minutes and for the pressure tests, pressure was applied to the center of the sensor with thumb pressure for 5 minutes: this simulates an interaction with a lump inside human breast tissue. Although the sensor is equipped for a 50.8 mm 8x8 grid and the DAQ system is expandable up to a 16x16 grid, a 6x6 grid was used for testing. A total of 36 data points was collected for each 200 milliseconds cycle. This was due to time constraints given by the effects of the virus.

I. RESULTS AND DISCUSSIONS

A prototype was successfully created using an EG-based sensor and 3D printed parts. This sensor was able to show the feasibility of such a device for sensing abnormalities in human breast tissue using an EG-sensor. The results of producing substantial sensing data had been limited because of the effects of the COVID-19 Corona virus that struck the world in the Spring and Summer of 2020.

The values seen at each cross point of the pressure map are the output voltage values of the sensor. At the points were no pressure is sensed, a value of zero (or near zero) is seen. This is because the resistance was not change and thus the input

0	0.54	0	0.54	0	0
0	0.54	0	0.54	0	0
0	0.54	0	0.54	0	0
0	0.54	0	0.54	0	0
0	0.55	0	0.55	0	0
0	0.49	0	0.49	0	0

Figure 3: Pressure map for first baseline test. Values of 0 mV (or near 0) assigned with green color display absence of pressure. This validates the baseline where there is no distinction in pressure.

10.69	10.72	10.18	9.65	10.19	10.72
10.72	10.76	10.22	9.68	10.22	10.76
12.36	12.40	11.85	11.32	11.86	12.40
10.14	10.18	9.64	9.11	9.64	10.18
21.42	21.49	20.93	20.39	20.94	21.49
1.47	1.48	0.99	0.49	0.99	1.48

Figure 4: Pressure map for first pressured test. Larger values (shown in red) display areas where pressure was detected. This test validates the ability of the sensor to detect pressures.

0.54	0.54	0	0	0	0
1.62	1.62	1.08	1.08	1.08	1.08
0.54	0.54	0	0	0	0
1.07	1.08	0.54	0.54	0.54	0.54
0.55	0.55	0	0	0	0
0	0	0.49	0.49	0.49	0.49

Figure 5: Pressure map of second baseline test. Values of 0 mV (or near 0) assigned with green color display absence of pressure. This test validates the ability of the EG-sensor to recover to its baseline steady state from first baseline test.

4.30	4.85	4.31	4.84	4.31	5.38
3.77	4.32	3.78	4.32	3.78	4.86
4.86	5.42	4.88	5.42	4.88	5.96
3.22	3.77	3.23	3.77	3.23	4.31
11.08	11.67	11.10	11.66	11.10	12.22
0.49	0.99	0.49	0.99	0.49	1.48

Figure 6: Pressure map of second pressured test. Larger values (shown in red) display areas where pressure was detected. This test validates the repeatability of the sensor and its ability to detect breast abnormalities by palpation.

voltage was the same as output, therefore the difference is zero. Where pressure was sensed the values were greater than zero. The resistance was increased, and the output voltage was increased therefore, the difference between input and output voltage is a positive value as seen on the pressure maps. The resistance changes were small, in the range of kiloohms, therefore the voltage differences were also small, in the range of millivolts. For these tests, the range of voltage values was between 0 and 30 mV as shown on the pressure maps.

Four pressure maps were created. Two baseline tests and two tests where pressure was applied. The first (Fig. 3) accurately displays the lack of pressure during the baseline test. The sensor was able to deliver data with no change in voltage. This creates a baseline pressure map where there is no distinction of pressure. This area is displayed in green.

The second test (Fig. 4) shows the detection of pressure at the center of the probe head. The whole sensing area detected some change in voltage (denoted in shades of green). This is because much of the probe head deforms when pressure is applied. The area of the sensor that encountered the most pressure detected areas of higher voltage change (denoted in red). This test and these results show the response and sensing capabilities of the sensor.

Although pressure was applied to the center of the sensor, the red area on the pressure map is skewed toward the bottom. This is because only a portion of the sensing grid was used (6x6 while the sensor is equipped for an 8x8 grid) since the first six rows of sensing strips were used, the data appears to be skewed toward the bottom of the pressure map while pressure is applied in the center. Understanding these results validates the locational accuracy of the pressure readings.

The third and fourth tests show the repeatability of the sensor function. These tests are shown in Fig. 5 & 6. Note the similarities between Fig. 3 & 5 (baseline tests) and between Fig. 4 & 6 (pressured tests). Since the two baseline test both reflect an absence of pressure, the repeatability of this test shows the ability of the sensor to recover to its original state. EG-sensors do take some time to return to a baseline steady state after encountering pressure. The similarities between the two pressure tests show the precision of the sensor: the sensor is able to repeat the same test while returning similar results.

II. CONCLUSION AND FUTURE WORKS

The research aims to aid breast diagnoses by creating a sensing probe to detect abnormalities and masses in human breasts. Clear detection brings a better chance at resolving the issue. To achieve this, the project manufactured a working prototype of an EG-based electrode sensing probe to palpate a breast and accurately detect abnormalities. A probe of this nature can be a less expensive alternative to ultrasound probes and other CBE techniques. An electrode-based sensing probe can also give different data such as tangible depth and size of a mass which may lead to a more accurate diagnosis. The probe may also be easier to operate than other technologies used today rendering it more attractive to smaller medical operations and lesser experienced technicians. With a working prototype, it will be easy to see the benefit and advantages it brings to the

medical field in an age where it is heavily populated with many different technologies. Finally, the research aids in solving an issue that kills an estimated 50,000 women each year in America [14].

An EG-based probe consisting of a flexible EG e-skin sensor, a 3D printed probe head, and a microcontroller was manufactured. The e-skin is constructed of a microwave exfoliated expanded graphite and latex solution that was sprayed onto a latex skin. The sensor is supported on the ABS printed probe head with silicone padding and is connected to the microcontroller via electrodes constructed of carbon braid and copper strand wire.

Although the probe created at this stage does demonstrate the feasibility of using EG-sensors for CBE, the prototype and research would like to be refined for future work. Future work includes the simplification of the manufacturing process. This was the lengthiest process of the development and require precision manufacturing with tools that were less than ideal. Although the production of a functioning prototype was achieved, in the future, better manufacturing techniques will be explored for a more refined prototype. This will be done continuously as it is the heart of R&D. It has also been noted that certain individuals possess allergic reactions to latex. Therefore, alternative materials will be explored to mitigate the exposure of this moderately allergic material.

As a by-product of refining the manufacturing process, an expanded senor will be produced. It has been concluded that a 63.5 – 76.2 mm (in diameter) sensor would be more ideal. This would create a larger sensing area for ease of palpation and allow for more sensing strips (expandable up to 16x16 grid by limitations of DAQ) and therefore provide more accurate sensing. Better accuracy needs to be applied to the voltage calculations and to the determination of the detected mass location. The improvements can mostly be made with help from sensor calibration.

The sensor should also be calibrated. Due to the effects and limitations of the COVID-19 virus, there was not sufficient time to properly calibrate the sensor. The sensor readings should be normalized over the length of the sensing strips. In addition, calibration for sensor recovery timing should be done. Both of these calibrations should improve the effectiveness, sensitivity, and ease of use of the sensor. These changes are software based. Once this has been done, more general testing to refine the function of the sensor and display its feasibility will be done. These tests will be done utilizing a full sensor grid (8x8 or larger). Such testing will be continued after the limitations of the virus are lifted. In the distant future, the development of the sensor may be handed off to other interested research parties.

The measurements produced by the sensor aid in determining the location, depth, and size of the mass. This is done electronically by displaying the readings on a visual map. During palpation, the user can physically note, on the breast, the location of a mass displayed by the sensors imaging. The depth can be read by the sight of the mass on the map. A deeper mass will exert less pressure and thus display accordingly on the map. A larger mass will appear on the map in the form of larger area.

This sensor cannot determine whether a detected mass is normal or abnormal. However, it is most commonly abnormal to have masses deep within the breast tissue. Once abnormalities are detected, further medical consideration should be taken.

Lastly, future work includes finalizing the development of an expandable data processing unit that includes *Bluetooth* capabilities. This unit will work in conjunction with and accompanying smartphone application for real time data processing. These works are nearing completion however, they have been halted - again - due to the impact of the virus.

Once these future considerations have been implemented, the goal is to be able to demonstrate further the feasibility and capabilities of such a sensor and market the prototype, and use of EG technology, to CBE and medical markets.

References

[1] T. Donica, J. Gray, and E. F. Zegeye, "Strain Mapping and Large Strain Measurement Using Biaxial Skin Sensors," in *ASME 2019 Conference on Smart Materials, Adaptive Structures and Intelligent Systems*, 2019, vol. ASME 2019 Conference on Smart Materials, Adaptive Structures and Intelligent Systems, V001T06A015.

[2] A. Riegel, J. Gray, and E. F. Zegeye, "Exfoliated-Graphite/Latex Piezoresistive System for Mapping Plantar Pressure," in *ASME 2019 Conference on Smart Materials, Adaptive Structures and Intelligent Systems*, 2019, vol. ASME 2019 Conference on Smart Materials, Adaptive Structures and Intelligent Systems, V001T06A014.

[3] E. M. Barnett, J. J. Lofton, M. Yu, H. A. Bruck, and E. Smela, "Targeted Feature Recognition Using Mechanical Spatial Filtering with a Low-Cost Compliant Strain Sensor," (in eng), *Sci Rep,* vol. 7, no. 1, p. 5118, Jul 11 2017.

[4] Y. He *et al.*, "A Novel Method for Fabricating Wearable, Piezoresistive, and Pressure Sensors Based on Modified-Graphite/Polyurethane Composite Films," (in eng), *Materials (Basel, Switzerland),* vol. 10, no. 7, p. 684, 2017.

[5] A. Mojra, S. Najarian, S. M. Kashani, and F. Panahi, "A novel tactile-guided detection and three-dimensional localization of clinically significant breast masses," (in eng), *J Med Eng Technol,* vol. 36, no. 1, pp. 8-16, Jan 2012.

[6] A. Mojra, S. Najarian, S. Kashani, and F. Panahi, "Artificial Tactile Sensing Capability Analysis in

Abnormal Mass Detection with Application in Clinical Breast Examination," *Proceedings of the World Congress on Engineering 2011, WCE 2011,* vol. 3, 07/01 2011.

[7] V. Landoni *et al.*, "Quantitative analysis of elastography images in the detection of breast cancer," *European Journal of Radiology,* vol. 81, no. 7, pp. 1527-1531, 2012/07/01/ 2012.

[8] J. Palacio-Torralba *et al.*, "Quantitative diagnostics of soft tissue through viscoelastic characterization using time-based instrumented palpation," *Journal of the Mechanical Behavior of Biomedical Materials,* vol. 41, pp. 149-160, 2015/01/01/ 2015.

[9] H. J. Pandya, R. Roy, W. Chen, M. A. Chekmareva, D. J. Foran, and J. P. Desai, "Accurate characterization of benign and cancerous breast tissues: Aspecific patient studies using piezoresistive microcantilevers," *Biosensors and Bioelectronics,* vol. 63, pp. 414-424, 2015/01/15/ 2015.

[10] M. Kujawski, J. D. Pearse, and E. Smela, "Elastomers filled with exfoliated graphite as compliant electrodes," *Carbon,* vol. 48, no. 9, pp. 2409-2417, 8// 2010.

[11] J. Wissman *et al.*, "New compliant strain gauges for self-sensing dynamic deformation of flapping wings on miniature air vehicles," *Smart Materials and Structures,* vol. 22, no. 8, p. 085031, 2013.

[12] A. T. Sepúlveda, R. G. D. Villoria, J. C. Viana, A. J. Pontes, B. L. Wardle, and L. A. Rocha, "Flexible Pressure Sensors: Modeling and Experimental Characterization," *Procedia Engineering,* vol. 47, pp. 1177-1180, 2012/01/01/ 2012.

[13] M. A. S. Mohammad Haniff *et al.*, "Piezoresistive effects in controllable defective HFTCVD graphene-based flexible pressure sensor," *Scientific Reports,* vol. 5, no. 1, p. 14751, 2015/10/01 2015.

[14] A. S. o. C. Oncology. (2020, April, 14). *Breast Cancer: Statistics*. Available: https://www.cancer.net/cancer-types/breast-cancer/statistics/2015